CHINESE JOURNAL OF PHYSICS VOL. 52, NO. 1-II February 2014

Review

Nuclear Fusion Driven by Coulomb Explosion of Deuterated Methane Clusters in an Intense Femtosecond Laser Field

Jiansheng Liu, Haiyang Lu, Zili Zhou, Cheng Wang, Hongyu Li, Changquan Xia, Wentao Wang, Yi Xu, Xiaoming Lu, Yuxin Leng, Xiaoyan Liang, Guoquan Ni, Ruxin Li, and Zhizhan Xu

State Key Laboratory of High Field Laser Physics, Shanghai Institute of Optics and Fine Mechanics, Chinese Academy of Sciences, P.O. Box 800-211, Shanghai 201800, China

(Received November 14, 2013)

We have made experimental studies on the generation of deuterium-deuterium fusion neutrons from intense Coulomb explosions (CE) of large-size $(CD_4)_N$ cluster jets under the irradiation of intense femtosecond laser pulses. By optimizing the propagation of a laser pulse in the cluster gas and the time delay between the laser pulse and the gas flow, the maximum neutron yield of 2.5×10^5, which corresponds to a conversion efficiency of 2.1×10^6 fusion neutrons per joule of incident laser energy, has been obtained with a 120-mJ, 60-fs laser pulse and cluster jets with an average molecular density of 3.6×10^{18} cm^{-3} and cluster radius of 7 nm. We have demonstrated that the neutron yields can be dramatically increased by using heteronuclear $(CD_4)_N$ clusters as compared with the similar sized homonuclear $(D_2)_N$ clusters. This enhancement is attributed to the significant increase in the deuteron kinetic energies due to energetic boosting and overrun effects during CE of heteronuclear clusters.

DOI: 10.6122/CJP.52.524 PACS numbers: 36.40.Gk, 52.50.Jm, 25.45.-z

I. INTRODUCTION

A cluster is a microscopic aggregation of 10^2–10^7 atoms (i.e., a few nanometers in radius) bound together by van der Waals forces. The interaction of a gas target composed of these kind of clusters with ultrashort intense laser pulses has attracted considerable attention in the last two decades since many fascinating phenomena have been observed such as strong absorption of laser energy, emission of laser harmonics, strong x-ray generation, and the production of very energetic and highly charged ions [1–3]. The latter has directly triggered the novel idea and implementation of table-top fusion neutron sources [4]. Possessing the properties of both solid and gas, clusters act as important targets which can bridge our knowledge of laser interaction with gas and solid. The generation of deuterium-deuterium (dd) fusion neutrons from Coulomb explosions of laser-heated clusters was firstly demonstrated by Ditmire *et al.* in 1999 and immediately arouse researchers' intense enthusiasm because just by irradiating cryogenic deuterium cluster jets with a low-energy, compact and high-repetition-rate table-top laser (35 fs, 150 mJ), an efficiency of about 10^5 fusion neutrons per joule of incident laser energy was achieved, which was close to the efficiency of large-scale laser-driven fusion experiments [4]. While blasting $(D_2)_N$ clusters with an

intense fs laser pulse, the electrons are stripped off the cluster, leaving the ions to explode violently from their mutual repulsion. The explosions are so violent that deuterons from neighboring clusters fuse and emit neutrons. Such kind of extremely short (sub-ns) bursts of fast neutrons could find wide applications in material science such as time-resolved study on radiation induced damage if the efficiency could be improved by 3 orders of magnitude [5, 6]. To that aim, quite a lot of work has been made to investigate the fusion dynamics in laser-cluster interactions, the characterization of fusion burn time and angular distribution of neutron emission, as well as to search for higher neutron yield [7–21]. The effects of the $(D_2)_N$ cluster size, the laser energies and focusing conditions have been investigated by Zweiback *et al.* to optimize the fusion neutron yields [8]. However, the average kinetic energies (KEs) of deuterons from explosion of $(D_2)_N$ clusters were reported to be located only in the range of 2.5–7 keV [7, 8, 14–16], which are still much lower than the optimal KEs in the range of 40–100 keV for efficient dd fusion.

Last and Jortner proposed an efficient mechanism for enhancing the deuterons' KEs by using clusters of heteronuclear deuterium containing molecules e.g. $(D_2O)_N$ and $(CD_4)_N$ [10, 11, 13, 17, 18]. For heteronuclear clusters, the light deuterons can outrun heavy ions inside the cluster and experience much more violent Coulomb repulsion due to energetic boosting effect and therefore the deuterons' KEs can be greatly enhanced. Moreover, a quasi-monoenergetic distribution of deuterons, suitable to induce dd fusion, can be generated due to this overrun effect. Our previous work has also indicated that the neutron yields from CD_4 clusters can be at least increased by 2 orders of magnitude compared with the same sized $(D_2)_N$ clusters [22]. In Ref. [13], Grillon *et al.* investigated the two origins of nuclear fusion driven by Coulomb explosion (NFDCE) of hetronuclear $(CD_4)_N$ clusters by using a low gas density of 2×10^{17} cm^{-3}. In their experiments, the most probable KE of D^+ ions could be as high as 45 keV with the estimated cluster size of 2×10^5 molecules (14.4 nm). This result indicated the significant enhancement of deuteron KEs by CE of $(CD_4)_N$ clusters as compared to $(D_2)_N$ clusters. However, Owing to the low gas density, the maximum neutron yield reported by them was ~ 8000 at a laser intensity of 7×10^{17} Wcm^{-2}, which corresponds to a conversion efficiency of 10^4 neutrons per joule of incident laser energy. It is much lower than the maximum neutron conversion efficiency (1×10^5/J) from NFDCE of $(D_2)_N$ clusters reported by Ditmire's group [4].

In Ref. [15], Madison *et al.* gave a comparison between the NFDCE of $(D_2)_N$ and $(CD_4)_N$ clusters. In their experiments, at low laser energy of 100 mJ, the fusion neutron yield in $(CD_4)_N$ clusters is higher than in $(D_2)_N$ clusters just by a factor of 2. However, by increasing laser energy from 100 mJ to 10 J, the neutron yield in $(CD_4)_N$ clusters became lower than that in $(D_2)_N$ clusters. They attributed this reversal in the actual fusion yield from expectation to a slight degradation in the jet performance, which produced a lower $(CD_4)_N$ gas jet density. Recently, we have successfully demonstrated that the neutron yields can be dramatically increased by 50 times by using heteronuclear $(CD_4)_N$ clusters in comparison with the similar sized homonuclear $(D_2)_N$ clusters [23, 24].

In the following, we have made experimental studies of generation of dd fusion neutrons from intense Coulomb explosions of high-density large-size $(CD_4)_N$ cluster jets under the irradiation of superintense femtosecond laser pulses. A correlated study of neutron

yields, deuterons' KEs and plasma channel formation diagnosed by a pump-probe interferometer allows us to optimize the coupling of laser-cluster interaction in order to produce very efficient nuclear fusion. The maximum efficiency of 2.1×10^6 fusion neutrons per joule of incident laser energy has been obtained with a 120-mJ, 60-fs laser and cluster jets with an average molecular density of 3.6×10^{18} cm^{-3} and cluster radius of 7 nm at a backing pressure of 84 bars. The comparison between $(D_2)_N$ and $(CD_4)_N$ clusters has been investigated with respect to the deuteron energy and neutron yield.

II. CLUSTER FORMATION AND DIAGNOSTICS

Although clusters can be produced in a number of ways, in laser-cluster interactions, clusters are generally produced by adiabatic expansion of gases through a conical nozzle into vacuum. When high-pressure gas flows into vacuum through a conical nozzle, due to adiabatic expansion these gaseous atoms or molecules cool and nucleate and can be held together by van der Waals forces into quite large-size clusters under appropriate conditions. As shown in Fig. 1(a), we have made a liquid nitrogen cooled pulsed valve to generate large-size clusters of deuterium or deuterated methane. Fig. 1 (b) shows a pulsed sonic gas jet with a conical nozzle. The throat diameter d is 310 mm, the length L is 26 mm, and the output diameter D is 4.5 mm. The operation repetition of the jet is 1 Hz and the vacuum is 2×10^{-3} Pa which is good for cluster formation. The onset of cluster formation and size estimation in gas jets can be characterized by a widely used empirical Hagena parameter [25–27]

$$\Gamma^* = k[d/\tan(\alpha)]^{0.85} p_0 T_0^{-2.29} \tag{1}$$

Where d is the diameter in μm of the jet throat, α is the half angle of the conical nozzle, p_0 is the backing pressure in mbar, T_0 is the initial gas temperature, and k is a constant that depends on the atomic species. The average number of atoms in a cluster is given as $< N >= 33(\Gamma^*/1000)^{2.35}$. The dependence of Hagena parameter on p_0 and T_0 indicates that high backing pressure and low gas temperature favors the production of large-size clusters. Although Hagena parameter gives a rough estimation of cluster formation and cluster size, it is not reliable to calculate the size of clusters generated by a gas jet by using Hagena parameter. In our experiment, Rayleigh scattering technique has been used to measure the intensity of scattering signal as a function of backing pressure and then the cluster size as function of backing pressure can be approximately calculated. Fig. 2 shows the measured scattering intensity of $(CD_4)_N$ clusters as a function of backing pressure from 10 to 80 bars. By a fitting procedure, the scattering intensity is proportional to P_0^4. At low pressure, we use the measured energy spectra of deuterons from laser-cluster interaction to calibrate the size of the $(CD_4)_N$ clusters [28]. The average size of $(CD_4)_N$ clusters at 80 bars is estimated to be 7 nm in radius.

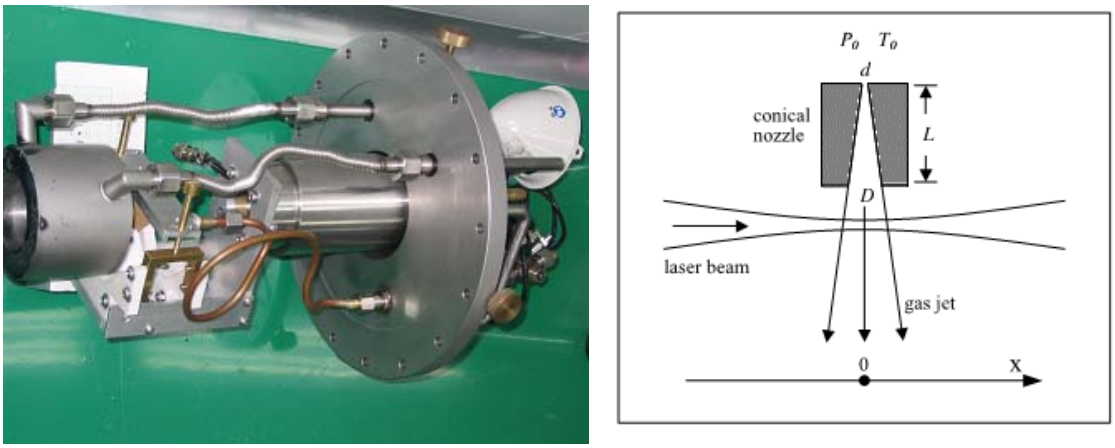

FIG. 1: Liquid nitrogen cooled pulsed valve and conical nozzle to generate large-size clusters of deuterium or deuterated methane.

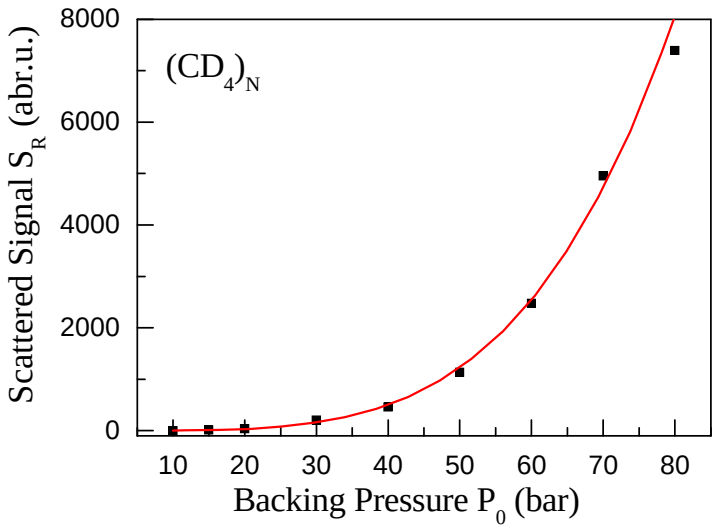

FIG. 2: Measured scattering signal of $(CD_4)_N$ clusters as a function of backing pressure from 10 to 80 bars.

III. EXPERIMENTAL SETUP FOR LASER-CLUSTER INTERACTION

The experimental setup is shown in Fig. 3. A chirped-pulse-amplification Ti:sapphire laser system deliveries 10-Hz laser pulses with the duration of 60 fs at the center wavelength of 800 nm into the chamber. The contrast ratio of the laser pulse is 10^7 on a time scale of 100

ps before the main pulse, preventing any pre-dissociation of the cluster in the experiments. The propagation effects of fs laser pulses in the cluster jets and the plasma channel formation are probed by splitting 5 percent of the laser beam and passing it perpendicularly across the plasma filament into a Michelson-type interferometer. The pump pulse which holds about 95% of the energy is tightly focused at 0.8 mm downstream from the nozzle exit by an $f/4$ off-axis parabolic mirror, yielding a maximum intensity of about $I_{peak} = 7 \times 10^{17}$ Wcm^{-2} (120 mJ) in vacuum. The focusing depth D_f (defined as the distance from the focal plane in vacuum to the gas jet axis) is arranged from -1.85 to 0.95 mm in order to investigate the propagation effect of incident laser, as well as to optimize the neutron production and KE of Deuterons. The neutrons are measured through a plastic scintillator coupled with a photomultiplier (PMT). Two detectors were used. One is home-made (ND-1), and calibrated by a neutron source in the institute of Chinese Academy of Engineering Physics (CAEP). The detection efficiency is calculated to be 0.31 pC per neutron, under the voltage supply of 2400 V. The other is bought from Saint-Gobian (BC-408), and the detection efficiency is measured according to ND-1 to be about 3.5 pC per neutron, under the voltage supply of 1200 V. The scintillator rod diameters are 127 mm and 180 mm for BC-408 and ND-1, respectively. The PMT was 2.5-ns fast response tube. The KEs of ions are measured through a 2.25-meter long time-of-flight spectrometer. Thanks to the high molecular polarizability of CD_4, large-size clusters can be produced even at room temperature by supersonic expansion of CD_4 gas into vacuum. However, in order to generate

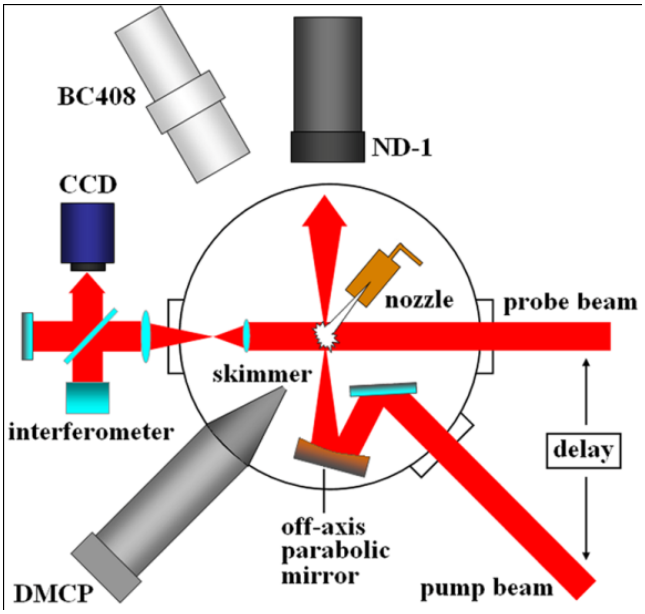

FIG. 3: Experimental setup for fusion neutron generation from laser-cluster interaction. The plasma channel formation is probed by splitting 5 percent of the laser beam and passing it perpendicularly across the plasma filament into a Michelson-type interferometer. The energy spectra of ions are measured through a 2.25-meter-long time-of-flight spectrometer.

large-size deuterium clusters, the pulsed solenoid valve has to be operated at liquid-nitrogen temperature.

IV. OPTIMIZATION OF NEUTRON GENERATION

In order to drive efficient dd nuclear fusion, highly energetic D^+ ions should be produced, which requires generation of large-size $(CD_4)_N$ clusters. On the other hand, efficient neutron generation greatly relies on the frequent collisions of D^+ ions, which requires a high deuteron density and the deposition of laser energy into the cluster jets should also be optimized. Therefore, the pulsed solenoid valve is designed to be operated at a high backing pressure of 80 bars. The opening of the valve is triggered by a square electric pulse with duration of 1.1 ms. However, the cluster flow can last several milliseconds. It must be mentioned that evolutions of gas density and the cluster size are quite different. The gas densities at the leading (small delay time) and tailing edges of the cluster flow are very low while the cluster size increases as the time delay increases. By changing the time delay between the laser pulse and the gas flow as well as the backing pressure, we have measured the interferograms of the plasma filaments, KEs of D^+ ions and neutron yields. Fig. 4 shows the typical interferograms of the plasma filaments at different time delays from 1.4 to 6 ms with a backing pressure of 80 bars. It can be seen that a long plasma channel with high electron density can be generated at a time delay of 3–4 ms. Using Abel inversion, the electron density as a function of plasma diameter at different positions along the plasma channel can be calculated. The D^+ ion density, which is half of the electron density if the average charge state of C^{4+} is produced, is calculated as a function of the time delay and shown in Fig. 5(a). It is found that the average deuteron density is around 1.2×10^{19} cm^{-3} at the time delays from 2 to 3.5 ms. In Fig. 5(a) we also show the measured average KEs of D^+ ions which increase rapidly from 4 to 13 keV as the time delay increases from 2 to 3.5 ms. However, the average KEs increase slowly from 13 to 15 keV and saturate as the time delay continues to increase. This increasing trend of average KEs implies the time-varying formation process of $(CD_4)_N$ clusters and the largest clusters are produced at the tailing edge of the cluster flow [29].

From Fig. 4 we can find that a plasma channel with a length of ~ 2 mm and radius of ~ 200 μm is produced only in the case of high-density cluster flow. It means that most of the laser energy is efficiently deposited into this plasma channel. The produced neutron yields at different time delays are simultaneously detected and shown in Fig. 5(b). The maximum yield of 2.5×10^5 neutrons is detected at 4 ms of delay with deuteron density of 1×10^{19} cm^{-3} and average KEs of 13.5 keV. Since the neutron yield is proportional to the squared density of the D^+ ions' and DD fusion cross section, the maximum neutron yield is determined by a trade-off between D^+ ions' density and average KEs. Considering the laser energy of 120 mJ, we have achieved a conversion efficiency of 2.1×10^6 neutrons per joule of incident laser energy, which is roughly higher by 2 orders of magnitude than the results reported by Madison and Grillon *et al.* [13, 14]. By increasing deuteron density through the increase of the backing pressures from 44 to 84 bars, we have measured neutron

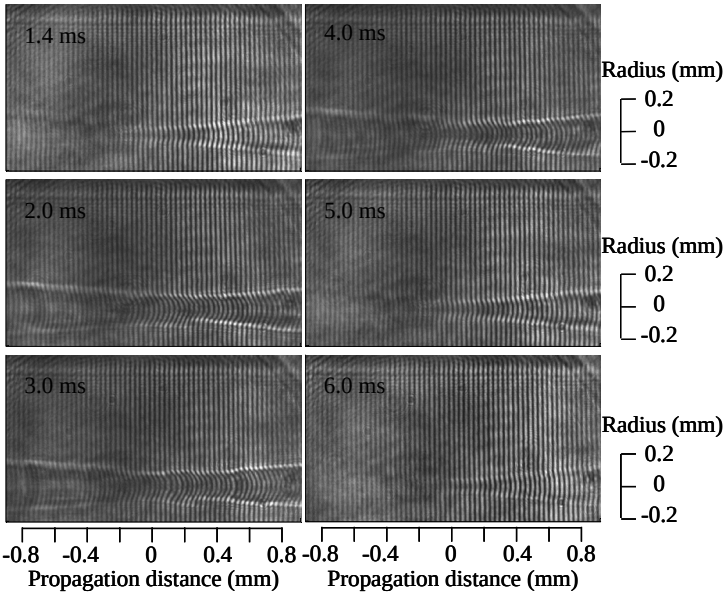

FIG. 4: Recorded interferograms of plasma filaments at different time delays from 1.4 to 6 ms.

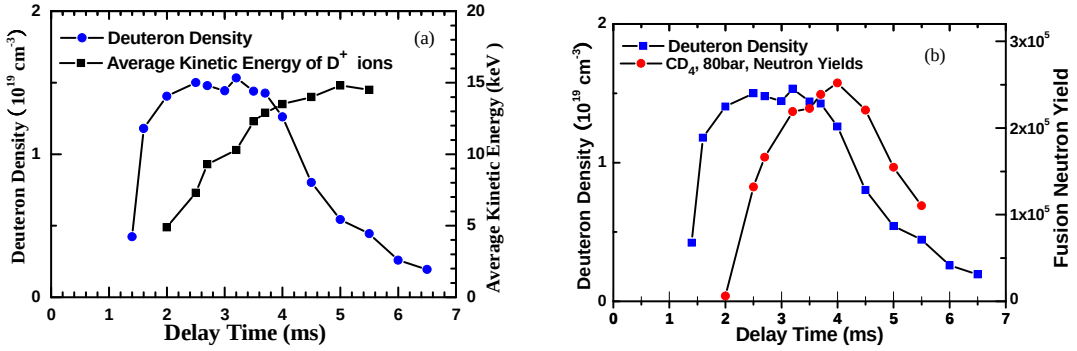

FIG. 5: Measured densities and average KEs of D^+ ions as a function of the time delay. (b) The measured densities of D^+ ions and neutron yields as a function of the time delay.

yields as a function of time delay at different backing pressure from 44 to 84 bars, which are shown in Fig. 6(a). The optimized neutron yields and D^+ ions' average KEs as a function of backing pressure are shown in Fig. 6(b). Although D^+ ions' average KEs are close to saturation as the backing pressure increases to 84 bars, we do not see the saturation effect of neutron yield. It means the efficiency of neutron generation can still be increased, e.g. by employing a cryogenic jet to produce larger-size cluster flows with higher gas densities.

On the other hand, efficient neutron generation relies on the optimal deposition of laser energy into the dense gas region. Because the low-density gas at the edge of the gas

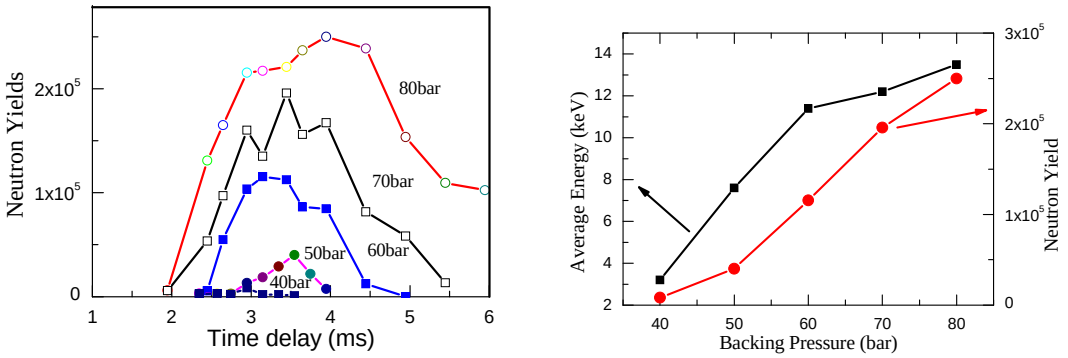

FIG. 6: Recorded interferograms of plasma filaments at different time delays from 1.4 to 6 ms. (b) Neutron yields as a function of time delay at different backing pressures from 40 to 80 bars.

jet can greatly absorb the laser energy and influence the generation of fusion neutrons, the propagation effect of femtosecond laser pulses in cluster gas such as the ionization-induced defocusing and absorption of the laser energy by the clusters should be considered [30]. By changing the focal position related to the center of the gas jet, the neutron yield as well as the KEs of D^+ can be optimized. The focusing depth D_f (defined as the distance from the focus plane to the gas jet axis) is arranged from -1.85 to 0.95 mm. Six typical interferograms of the filaments and the non-axisymmetric-Abel-inverted electron density distributions are listed in Fig. 7 [31]. Here, the laser energy is 80 mJ, and the pulse duration is 60 fs. The maximum electron density is estimated to be 2.88×10^{19} cm^{-3} as shown in Fig. 7, so the neutral $(CD_4)_N$ gas density is approximated to be 3.6×10^{18} cm^{-3} provided that C^{4+} is the highest ionization state in this condition Simultaneously detected neutron yields, average KEs of D^+ ions and N_D+ (total number of D^+ ions within filament) are shown in Fig. 8

Two evident phenomena are observed in Fig. 7: the plasma filament length is restricted within 2.5 mm due to the laser attenuation; and the filament shape is modified by the ionization-induced defocusing effect. When D_f is -1.85 and -1.55 mm as shown in Fig. 7(a) and 7(b), the filament with a conic shape is confined at edge of the gas jet. Large waist of the filament near the jet axis suggests low laser intensity, which leads to low KEs of the D^+ ions and thus limited neutron yields not exceeding 4.5×10^4 per shot as shown in Fig. 7(b). As focusing the laser pulse deeper into the gas jet with D_f being -0.95 and -0.60 mm as shown in Fig. 7(c) and 7(d), the plasma defocusing effect starts to counteract the convergence of incident beam and results in a cylindrical-shaped plasma channel with a constant small diameter. Although N_D^+ is at low level as shown in Fig. 7(b), the KE of D^+ ions increases and obtains the maximum value of 17 keV when D_f increases to -0.60 mm. Simultaneously, the maximum neutron yield of 1.9×10^5 neutrons per shot is obtained in this case. When D_f increases further to -0.05 and 0.45 mm as shown in Fig. 7(e) and 7(f), the filament holds a swelled volume deep in the jet, resulting in obviously growing N_D^+ as

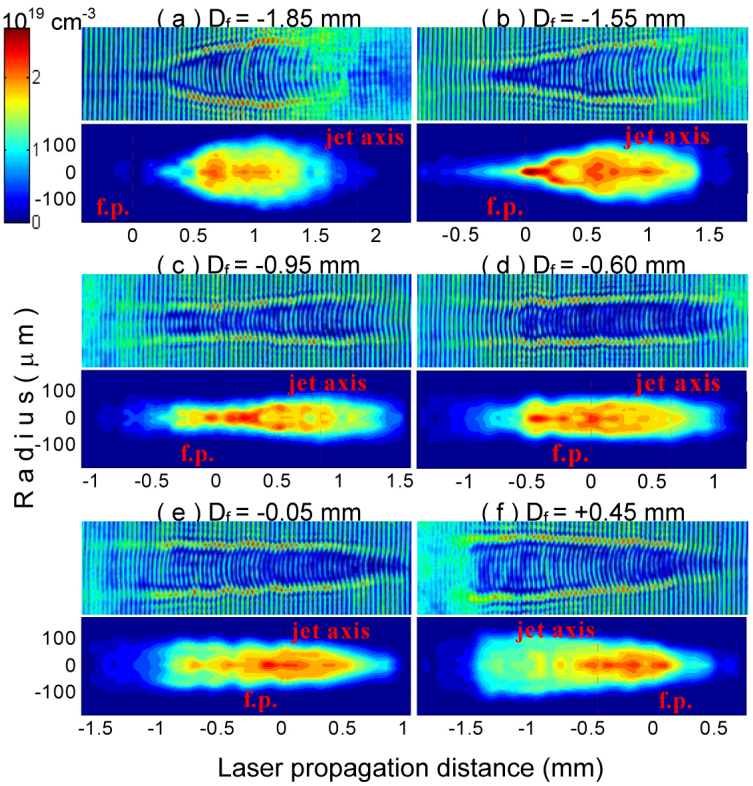

FIG. 7: Interferograms of the plasma filaments at the backing pressure of 84 bars for six typical D_f s (from -1.85 to 0.45 mm) and the non-asymmetric-Abel-inverted electron density distributions. The locations of focal plane (f. p.) and gas jet axis are marked by dashed lines. The laser pulse propagates from the left to the right of the images.

shown in Fig. 8. However, the neutron yields decline by a large margin because most of the D^+ ions within the filament are less energetic owing to the weakened laser intensity caused by the greater laser absorption.

V. COMPARISON BETWEEN $(D_2)_N$ AND $(CD_4)_N$ CLUSTERS

As a comparison, we have measured the D^+ ion energy spectrum and neutron yield generated from the Coulomb explosion of $(D_2)_N$ clusters. The $(D_2)_N$ clusters are produced by using a supersonic gas jet, cryogenically cooled with liquid nitrogen at 100 K. At a backing pressure of 64 bars, the average cluster radius is estimated to be about 6 nm. The measured energy spectrum of D^+ ions is shown in Fig. 9(a). Also shown is the energy spectrum of D^+ ions from $(CD_4)_N$ cluster experiment at 84 bars of backing pressure and the average cluster size is estimated to be 7 nm. The average/maximum KEs of D^+ ions are 3.6 keV / 14.45 keV and 13.4 keV / 60 keV for $(D_2)_N$ and $(CD_4)_N$ clusters, respectively. The

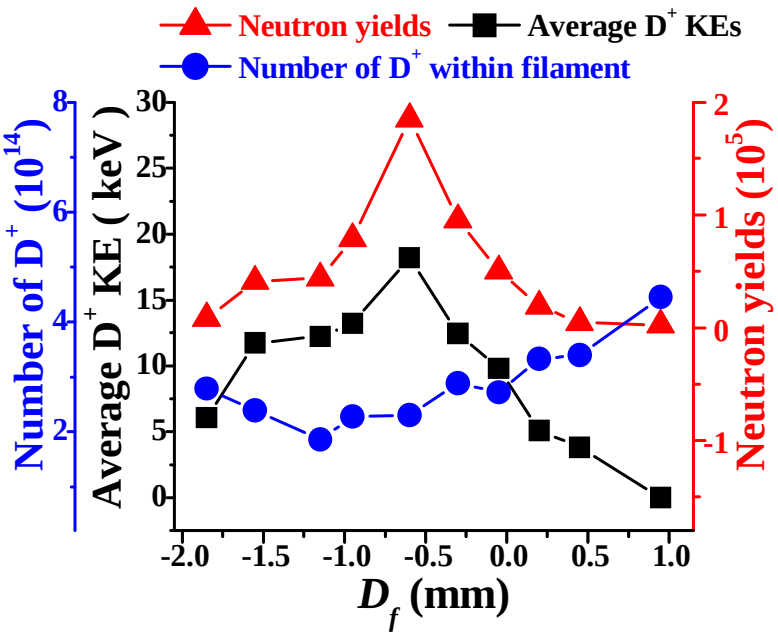

FIG. 8: Measured neutron yields, average KEs of deuterons and N_D+s (total number of deuterons within filament) for different D_f s (from −1.85 to 0.95 mm).

maximum and average KEs of D^+ ions from $(CD_4)_N$ clusters are both increased by 3 times, compared with D_2 clusters with the similar radius. This enhancement shows explicitly the contribution of both the energetic boosting and the kinematic effects in the CE of the heteronuclear clusters [22, 32]. For the $(D_2)_N$ and $(CD_4)_N$ clusters, we detect the fusion neutron yield of 5×10^3 and 2.5×10^5 per pulse which corresponds to the efficiencies of 4×10^4 and 2.1×10^6 neutrons per joule of incident laser energy. The neutron yield is dramatically increased by 50 times, without considering the relatively low deuteron density of $(CD_4)_N$ clusters compared with the cryogenically cooled $(D_2)_N$ clusters. Fig. 9(b) shows the measured neutron yields from $(D_2)_N$ and $(CD_4)_N$ clusters respectively as a function of backing pressure from 44 to 84 bars.

A modified model based on the Coulomb explosion model is proposed to roughly estimate the nuclear fusion yields produced in the Coulomb explosion of $(D_2)_N$ and $(CD_4)_N$ clusters with irradiation of the intense laser pulses, by taking the attenuation of laser energy absorbed by the clusters with a log-normal size distribution into account [22, 33]. The neutron yield generated inside the heated plasma filament, as the sum of the intercluster fusion yield and beam-target fusion yield, is calculated as a function of laser-cluster parameters such as the cluster size, the laser energy, the focus spot radius and position. Only these parameters match with each other, can the neutron yield or the neutron conversion efficiency be maximized.

A comparison between the contribution of heteronuclear and homonuclear clusters to the fusion yield is made between $(CD_4)_N$ and $(D_2)_N$ with equal size R_0. Because of

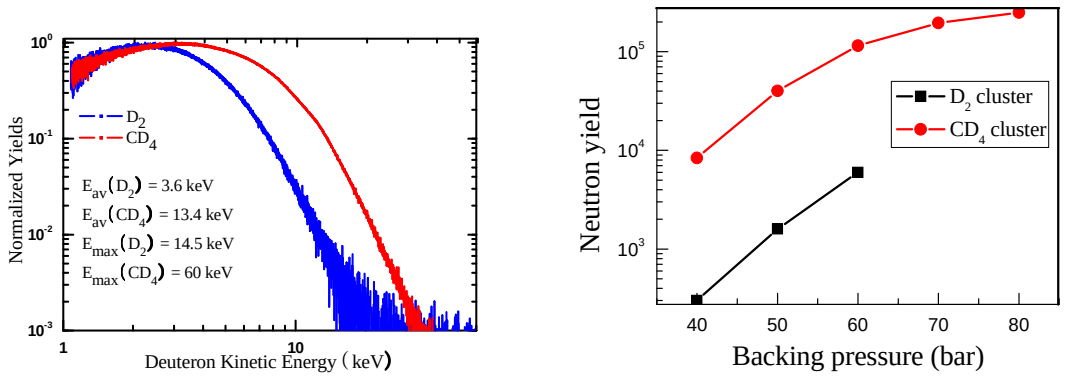

FIG. 9: (a) Measured energy spectrum of D^+ ions from $(D_2)_N$ and $(CD_4)_N$ clusters, respectively. (b) Measured neutron yields from $(D_2)_N$ and $(CD_4)_N$ clusters respectively as a function of backing pressure from 44 to 84 bars.

the boosting effect of multicharged carbon ions on the kinetic energy of deuterons and the accelerating effect on the deuteron velocity in the overrun process of deuterons relative to heavy carbon ions, the deuteron energy of $(CD_4)_N$ is highly increased compared to that of $(D_2)_N$ with the same cluster size. For example, the maximum and average deuteron energies of the $(CD_4)_N$ cluster are respectively 3.2 times and 4.6 times as high as those of the $(D_2)_N$ cluster. Furthermore in the energy spectrum of $(CD_4)_N$, a large number of deuterons locate close to the maximal energy due to the overrun effect of deuterons relative to heavy carbon ions, which facilitates high fusion efficiency. The dependence of nuclear reaction yield originating from Coulomb explosion of the two kinds of clusters on the cluster radius is presented in Fig. 10. The fusion yield increases conspicuously as the initial cluster size increases. For smaller cluster which produces lower deuteron energy, the beam-target reaction yield Y_{bt} is lower than the intercluster fusion yield Y_{ic}. As the cluster size increases, Y_{bt} becomes comparable to Y_{ic}. Eventually Y_{bt} exceeds Y_{ic} with further increase of cluster size. A clear relationship is obtained from the figure that the intercluster and beam-target *dd* fusion yield as well as the total fusion yield of $(CD_4)_N$ are accordingly improved by a magnitude of one or two orders compared to those of $(D_2)_N$ with the same cluster size. A qualitative agreement is obtained between our simulated and the measured results. It has been validated that heteronuclear clusters are a better candidate compared to homonuclear clusters for enhancing the total intercluster fusion yield because both a higher energy region and a higher proportion of deuterons distributing in the energy region can be created in the deuterated heteronuclear clusters.

In conclusion, we have experimentally demonstrated efficient generation of dd fusion neutrons from intense Coulomb explosions of high-density large-size $(CD_4)_N$ cluster jets under the irradiation of superintense femtosecond laser pulses. A correlated study of neutron yields, deuterons' kinetic energies and plasma channel formation diagnosed by a

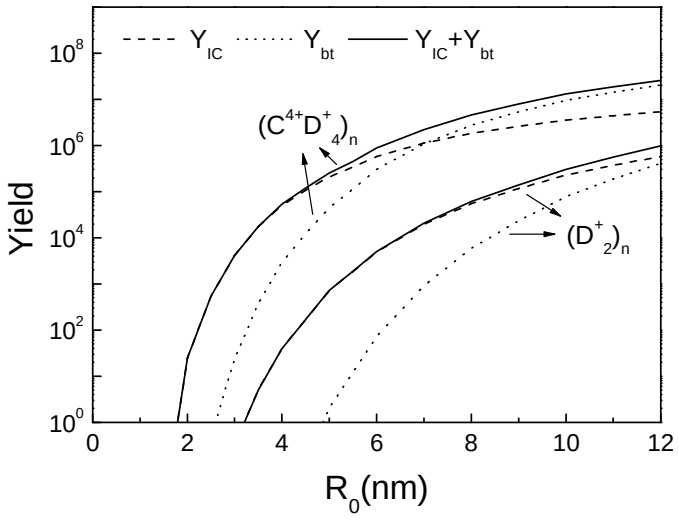

FIG. 10: Dependences of the nuclear reaction yield originating from cluster Coulomb explosion of $(CD_4)_N$ and $(D_2)_N$ on the cluster radius R_0. The dash, dot, solid lines represent the intercluster, beam-target and total fusion yield respectively.

pump-probe interferometer allows us to optimize the coupling of laser-cluster interaction in order to produce efficient nuclear fusion. By adjusting the time delay between the laser pulse and gas flow as well as the focusing condition, the neutron yield can be significantly increased. The comparison between $(D_2)_N$ and $(CD_4)_N$ clusters has been investigated with respect to the deuteron energy and neutron yield. It has been verified that the neutron yields can be dramatically increased by using heteronuclear $(CD_4)_N$ clusters as compared with the similar sized homonuclear $(D_2)_N$ clusters. This enhancement is attributed to the significant increase in the deuteron kinetic energies due to energetic boosting and overrun effects during CE of heteronuclear clusters.

This work was supported by the National Basic Research Program of China (Contract No: 2010CB923203, 2011CB808100), National Natural Science Foundation of China (Contract Nos: 11127901, 61221064, and 10974214), Shanghai science and technology talent project (12XD1405200), the State Key Laboratory Program of Chinese Ministry of Science and Technology, and the Cooperation in the Development and Application of Femtosecond Petta-watt Level Ultra-intense and Ultra-short Laser System (Grant No. 2011DFA11300).

References

[1] T. Ditmire *et al.*, Nature **386**, 54 (1997).

[2] A. McPherson *et al.*, Phys. Rev. Lett. **72**, 1810 (1994).
[3] J. S. Liu, R. X. Li, P. P. Zhu, Z. Z. Xu, and J. R. Liu, Phys. Rev. A **64**, 033426 (2001).
[4] T. Ditmire *et al.*, Nature **398**, 489 (1999).
[5] A. Almazouzi, *et al.*, J. Nucl. Mater. **251**, 291 (1997).
[6] T. Ditmire, *et al.*, Rad. Phys. and Chem. **70**, 535 (2004).
[7] J. Zweiback *et al.*, Phys. Rev. Lett. **84**, 2634 (2000).
[8] J. Zweiback *et al.*, Phys. Rev. Lett. **85**, 3640 (2000).
[9] P. B. Parks, T. E. Cowan, R. B. Stephens, and E. M. Campbell, Phys. Rev. A **63**, 063203 (2001).
[10] I. Last and J. Jortner, Phys. Rev. A **64**, 063201 (2001).
[11] I. Last and J. Jortner, Phys. Rev. Lett. **87**, 033401 (2001).
[12] I. Last and J. Jortner, J. Phys. Chem. A **106**, 19877 (2002).
[13] G. Grillon *et al.*, Phys. Rev. Lett. **89**, 065005 (2002).
[14] K. W. Madison, Pravesh K. Patel, Matt Allen, Dwight Price, and T. Ditmire, J. Opt. Soc. Am. **20**, 113 (2003).
[15] K. W. Madison *et al.*, Phys. Plasmas **11**, 270 (2004).
[16] K. W. Madison *et al.*, Phys. Rev. A **70**, 053201 (2004).
[17] I. Last and J. Jortner, J. Chem. Phys. **121**, 8329 (2004).
[18] A. Heidenreich, J. Jortner, and I. Last, Proceed. Natl. Acad. Sci. USA **103**, 10589 (2006).
[19] I. Last and J. Jortner, Phys. Rev. Lett. **97**, 173401 (2006).
[20] I. Last and J. Jortner, Phys. Rev. A **77**, 033201 (2008).
[21] I. Last, S. Ron, A. Heidenreich, and J. Jortner, High Power Laser Science and Engineering **2**, 69 (2013)
[22] H. Y. Li *et al.*, J. Phys. B **40**, 3941 (2007).
[23] H. Y. Lu *et al.*, Phys. Plasmas **16**, 083107 (2009).
[24] H. Y. Lu *et al.*, Phys. Rev. A (R) **80**, 051201 (2009).
[25] O. F. Hagena and W. Obert, J. Chem. Phys. **56**, 1793 (1972).
[26] O. F. Hagena, Z. Phys. D: At. Mol. Clusters **4**, 291 (1987).
[27] O. F. Hagena, Rev. Sci. Instrum. **63**, 2374 (1992).
[28] G. L. Chen *et al.*, J. Phys. B **40**, 445 (2007).
[29] W. T. Wang *et al.*, Laser Phys. **19**, 974 (2009).
[30] Z. L. Zhou *et al.*, J. Phys. B: At. Mol. Opt. Phys. **43**, 135603 (2010).
[31] P. Tomassini and A. Giulietti, Opt. Commun. **199**, 143 (2001).
[32] S. Li *et al.*, Chin. Opt. Lett. **11** (s), s23501 (2013).
[33] H. Y. Li *et al.*, Phys. Rev. A **79**, 043204 (2009).